The effect of co-operative Jahn-Teller interactions on C_{60}^{-} anions

Elie A. Moujaes and Janette L. Dunn‡

School of Physics and Astronomy, University of Nottingham, Nottingham, NG7 2RD, UK.

Abstract. Singly-charged buckminster fullerene anions, C_{60}^{-}, are subject to a strong intramolecular $T \otimes h$ Jahn-Teller (JT) effect. When such ions interact with other C_{60}^{-} ions in a solid through a co-operative JT effect, they will be subject to an additional interaction. There are a number of different mechanisms that can cause this interaction. However, in the molecular field approximation, all can be modelled phenomenologically in terms of a symmetry-lowering interaction written in terms of a linear combination of electronic operators for the h modes involved in the intramolecular JT effect. We will consider the combined effect of this distortion and the intramolecular JT effect. We will analyse the lowest adiabatic potential energy surface, and calculate the energies of the resultant vibronic states. The results are shown to have a complicated dependence on the particular combination of h modes chosen, and the energies of the resultant vibronic states can not easily be deduced from the form of the potential alone.

PACS numbers: 71.70.Ej,61.48.-c

Submitted to: *J. Phys.: Condens. Matter*

‡ email: Janette.Dunn@nottingham.ac.uk

1. Introduction

Solids formed by combining C_{60} fullerene molecules and alkali metals to form solids of the type A_nC_{60} (n = 1 to 6) have a number of unusual and intriguing physical properties. A_3C_{60} solids show unexpected conducting and superconducting properties [1, 2, 3], with K_3C_{60} being superconducting at temperatures below 18K, Rb_3C_{60} below 28K and Cs_3C_{60} below 47K [4]. In contrast, A_4C_{60} compounds are insulators. AC_{60} compounds form a polymeric structure in ambient conditions, with RbC_{60} and CsC_{60} undergoing a metal-insulator phase transition at $T_c \sim 50$ K and $T_c \sim 40$ K respectively [5, 6, 7].

The structure of A_nC_{60} solids can also vary. Many of these materials are face centred cubic (fcc) structures, but some are body centred tetragonal (bct) and body centred cubic (bcc) structures. The low temperature structure of AC_{60} is orthorhombic with an unusually short separation of 9.1Å- 9.4Å between the centres of C_{60} molecules along one of the crystallographic directions [8]. In addition, amorphous-carbon structures based on linearly polymerized C_{60} molecules have been found under a pressure above 5 GPa [9, 10]. In a cluster of A_3C_{60} molecules at room temperature, when the fcc solid form of C_{60} is maintained, the molecules rotate randomly about their lattice positions between different orientations. In fact the rotational levels are much closer to each other than the vibrational levels, meaning that the molecules populate the rotational levels much more easily. However, at temperatures lower than 261K, two of the rotational degrees of freedom freeze out, resulting in a lowering of symmetry and merohedral order [11, 12]. Similar conclusions have also been found in compounds containing C_{60}^{2-} ions [13].

Influence of the vibrational motion of the C_{60} molecule on the electronic motion is known to be important in these fullerene systems. Isolated fullerene ions C_{60}^{n-} (n = 1 to 5) are subject to an intramolecular Jahn-Teller (JT) effect of the form $T \otimes h$, where a triply degenerate electronic state T is coupled to a five dimensional vibrational mode h [14]. The JT effect causes an instantaneous distortion of the icosahedral C_{60} cage to a lower symmetry. However, there are a number of different distorted configurations all having the same energy. Quantum-mechanical tunnelling between the equivalent configurations restores the icosahedral symmetry in the dynamical JT effect. However, to understand the properties of fullerene solids, it is necessary to go beyond studies of isolated fullerene centres and to consider interactions between fullerene centres and/or interactions with a surface. There are various possible mechanisms for producing interactions between C_{60} ions in C_{60} solids. One factor which is believed to play a major role in determining the contrasting behavior of A_3C_{60}, A_4C_{60} and AC_{60} compounds is the co-operative JT (CJT) interaction between the different ions [15]. As a result of the CJT effect, different possible JT distortions are no longer equivalent and so the dynamical JT effect does not prevail in the lattice. JT distortions of individual centres can be locked in place and in general the lattice configuration will consist of a periodic arrangement of statically distorted ions [16].

Various correlation mechanisms have been proposed to describe the co-operative

interactions between JT centres, some of which involve phonons and some of which do not. In all cases, the interaction Hamiltonian $\mathcal{H}_{ij}$ between centres i and j can be represented phenomenologically (independent of the mechanism involved) using terms quadratic in the collective displacements $Q_{i\lambda}$ and $Q_{j\lambda}$ of the vibrationally-coupled modes λ at sites i and j, or equivalently a form quadratic in the electronic operators $\sigma_{i\lambda}$ and $\sigma_{j\lambda}$ used to describe the intramolecular JT interaction at sites i and j [15, 16]. One way to proceed is to then use the molecular field approximation. After making some appropriate transformations, this results in a mean-field Hamiltonian $\mathcal{H}_i^{mf}$ for site i which is equivalent to the intramolecular JT Hamiltonian for site i plus an additional contribution $\mathcal{H}_s = -\sum_\lambda w_\lambda \sigma_\lambda$, where the w_λ are constants whose values depend on the form of the interaction [16, 17]. The result for centre i is the same Hamiltonian as would be used for an intramolecular JT effect plus an additional symmetry-lowering distortion. The latter is sometimes referred to as a 'strain', although the origin of this term will not be that of an external stress on the system [15].

In this paper, we will be concerned with JT effects experienced by fullerene anions C_{60}^-. From group theory, coupling of isolated ions to two a_g and eight h_g vibrational modes is allowed. However, the coupling to the a_g modes does not have any significance, and for most purposes the coupling to the eight h_g modes can be replaced by coupling to a single effective mode [18]. Therefore, the relevant intramolecular JT effect for C_{60}^- is a $T_{1u} \otimes h_g$ system [14]. The nuclear coordinates Q_λ thus correspond to the vibrational mode h_g. By convention, the components λ are denoted by $\{\theta, \epsilon, 4, 5, 6\}$ [19]. We will consider a linear intramolecular JT effect subject to an additional symmetry-lowering distortion that can be written in terms of the electronic operators σ_λ relevant to the h mode in this system. The distortion can act along the direction of any one of the components λ, or along a linear combination of these directions. We will analyse the shape of the lowest adiabatic potential energy surface (LAPES) in different situations in order to understand the effect of the direction of the distortion, and investigate how the energies of the resultant vibronic states vary with the magnitude and direction of the distortion.

2. The Hamiltonian

The total Hamiltonian of a linear $T \otimes h$ JT system subject to an additional symmetry-lowering interaction $\mathcal{H}_s$ is $\mathcal{H} = \mathcal{H}_{vib} + \mathcal{H}_{int} + \mathcal{H}_s$, where $\mathcal{H}_{vib}$ and $\mathcal{H}_{int}$ are vibrational and electron-phonon interaction terms respectively, given by

$$\begin{aligned} \mathcal{H}_{vib} &= \frac{1}{2} \sum_\nu \left(\frac{P_\lambda^2}{\mu} + \mu \omega_H^2 Q_\lambda^2 \right) \sigma_o \\ \mathcal{H}_{int} &= k_H \sum_\lambda Q_\lambda \sigma_\lambda. \end{aligned} \tag{1}$$

λ is summed over the five vibrational degrees of freedom $\{\theta, \epsilon, 4, 5, 6\}$. Q_ν and P_λ are the collective coordinates and their conjugate momenta respectively. k_H is the linear JT coupling constant, μ is the reduced mass of the system and ω_H is the frequency

of vibration. σ_o is the identity matrix in three dimensions. Explicitly, we can write [14, 20, 21]

$$\mathcal{H}_{int} = \frac{k_H}{2} \begin{pmatrix} Q_\theta - \sqrt{3}Q_\varepsilon & -\sqrt{3}Q_6 & -\sqrt{3}Q_5 \\ -\sqrt{3}Q_6 & Q_\theta + \sqrt{3}Q_\varepsilon & -\sqrt{3}Q_4 \\ -\sqrt{3}Q_5 & -\sqrt{3}Q_4 & -2Q_\theta \end{pmatrix} \tag{2}$$

from which the definitions of the electronic interaction matrices σ_λ can be deduced. When defined in this manner, k_H is equivalent to the coupling constant k of Ref. [14], and is related to the constant V_H used in Ref. [21] by the relation $k_H = -2V_H/\sqrt{10}$.

2.1. Separation of coordinates

When linear JT effects only are included in the $T \otimes h$ problem, the LAPES contains a four-dimensional trough of equivalent-energy points. The motion of a system subject to this JT effect will consist of vibrations across and rotations of a distortion around the trough, often called pseudorotations. These should not be confused with the real rotations of the molecule. The trough has SO(3) symmetry, which is accidentally higher than the I_h symmetry expected for the $T \otimes h$ problem. Due to this symmetry, it is useful to write the Q_λ in the polar form [14, 20]

$$\begin{aligned}
Q_\theta &= \rho \left(\frac{1}{2}(3\cos^2\theta - 1)\cos\alpha + \frac{\sqrt{3}}{2}\sin^2\theta \sin\alpha \cos 2\gamma \right) \\
Q_\epsilon &= \rho \left(\frac{\sqrt{3}}{2}\sin^2\theta \cos 2\phi \cos\alpha - \cos\theta \sin 2\phi \sin\alpha \sin 2\gamma \right. \\
&\qquad \left. + \frac{1}{2}(1+\cos^2\theta)\cos 2\phi \sin\alpha \cos 2\gamma \right) \\
Q_4 &= \rho \left(\frac{\sqrt{3}}{2}\sin 2\theta \sin\phi \cos\alpha - \frac{1}{2}\sin 2\theta \sin\phi \sin\alpha \cos 2\gamma - \sin\theta \cos\phi \sin\alpha \sin 2\gamma \right) \\
Q_5 &= \rho \left(\frac{\sqrt{3}}{2}\sin 2\theta \cos\phi \cos\alpha - \frac{1}{2}\sin 2\theta \cos\phi \sin\alpha \cos 2\gamma + \sin\theta \sin\phi \sin\alpha \sin 2\gamma \right) \\
Q_6 &= \rho \left(\frac{\sqrt{3}}{2}\sin^2\theta \sin 2\phi \cos\alpha + \cos\theta \cos 2\phi \sin\alpha \sin 2\gamma \right. \\
&\qquad \left. + \frac{1}{2}(1+\cos^2\theta)\sin 2\phi \sin\alpha \cos 2\gamma \right),
\end{aligned} \tag{3}$$

where ρ is the radial distance, (θ, ϕ, γ) are Euler angles, and α is an extra angle to complete the five dimensional Q-space. [14, 20] For all points to be included once only, we can choose $0 \leq \rho < \infty$, $0 \leq \phi \leq 2\pi$, $0 \leq \theta \leq \pi$, $0 \leq \gamma \leq 2\pi$ and $0 \leq \alpha < \pi/3$.

It is also useful to rewrite the Hamiltonian $\mathcal{H}$ in a rotating coordinate frame by multiplying by a rotation matrix $\mathcal{R}(\gamma, \theta, \phi)$ [20, 14] such that the rotated interaction

Hamiltonian $\widetilde{\mathcal{H}}_{int} = R\mathcal{H}_{int}R^{-1}$ takes the diagonal form

$$\widetilde{\mathcal{H}}_{int} = \frac{k_H\rho}{2}\begin{pmatrix} \cos\alpha - \sqrt{3}\sin\alpha & 0 & 0 \\ 0 & \cos\alpha + \sqrt{3}\sin\alpha & 0 \\ 0 & 0 & -2\cos\alpha \end{pmatrix}. \tag{4}$$

From this, it can be seen that the lowest eigenvalue is lowest of all when $\alpha = 0$. [14] Also, the eigenvalue is independent of the angles θ, ϕ and γ, which is consistent with the interpretation of the LAPES being a trough.

If we explicitly write $P_\lambda = -\mathrm{i}\hbar\ \partial/\partial \mathrm{Q}_\lambda$, the vibrational Hamiltonian in the five-dimensional polar coordinates becomes

$$\mathcal{H}_{vib} = \left[-\frac{\hbar^2}{2\mu\rho^2}\frac{\partial}{\partial\rho}\left(\rho^2\frac{\partial}{\partial\rho}\right) + \frac{1}{2}\mu\omega_H^2\rho^2 + \frac{\hat{L}^2}{6\mu\rho^2}\right]\sigma_o \tag{5}$$

where $\hat{L}^2$ is the usual angular momentum operator

$$\hat{L}^2 = -\hbar^2\left[\frac{1}{\sin\theta}\frac{\partial}{\partial\theta}\left(\sin\theta\frac{\partial}{\theta}\right) + \frac{1}{\sin^2\theta}\frac{\partial^2}{\partial\phi^2}\right]. \tag{6}$$

The transformed Hamiltonian for the additional distortion $\mathcal{H}_s$ is a complicated result involving θ, ϕ and γ. However, we can make the approximation that mixing between the different APESs due to the additional distortion can be neglected. This gives us the contributions

$$\begin{aligned} W_\theta &= \frac{1}{4}w_\theta(1 + 3\cos 2\theta) \\ W_\epsilon &= \frac{\sqrt{3}}{2}w_\epsilon\sin^2\theta\cos 2\phi \\ W_4 &= \frac{\sqrt{3}}{2}w_4\sin 2\theta\sin\phi \\ W_5 &= \frac{\sqrt{3}}{2}w_5\sin 2\theta\cos\phi \\ W_6 &= \frac{\sqrt{3}}{2}w_6\sin^2\theta\sin 2\phi \end{aligned} \tag{7}$$

from each of the component ν. Therefore, the equation that gives the LAPES takes the form

$$\left[-\frac{\hbar^2}{2\mu\rho^2}\frac{\partial}{\partial\rho}\left(\rho^2\frac{\partial}{\partial\rho}\right) + \frac{\hat{L}^2}{6\mu\rho^2} + U_{\mathit{eff}}\right]\Psi_g = E_g\Psi_g \tag{8}$$

where Ψ_g and E_g are the rovibronic (rotational+vibronic) wave function and the energy of the LAPES respectively and U_{eff} is the effective potential

$$U_{\mathit{eff}} = \frac{\mu\omega_H^2}{2}\rho^2 - k_H\rho + \sum_\lambda W_\lambda. \tag{9}$$

The wave function Ψ_g at a given point $(\rho, \theta, \phi, \gamma)$ can be written as a product of electronic (ψ_g), vibrational (χ) and rotational wave functions (ψ_R)

$$\Psi_g = \psi_g(\theta, \phi) \times \chi(\rho) \times \psi_R(\theta, \phi), \tag{10}$$

where we already know that [21]

$$\psi_g(\theta,\phi) = \begin{pmatrix} \sin\theta\cos\phi \\ \sin\theta\sin\phi \\ \cos\theta \end{pmatrix}. \tag{11}$$

The vibrational wave function then satisfies the equation [21]

$$\left[-\frac{\hbar^2}{2\mu}\frac{\partial^2}{\partial\rho^2} - \frac{\hbar^2}{\mu\rho}\frac{\partial}{\partial\rho} + \frac{1}{2}\mu\omega_H^2\rho^2 - k_H\rho\right]\chi(\rho) = E_{vib}\chi(\rho). \tag{12}$$

and the rotational part is governed by the equation

$$\left(\frac{\hat{L}^2}{6\mu\rho^2} + W_\nu\right)\psi_R(\theta,\phi) = E_R\psi_R(\theta,\phi). \tag{13}$$

Equations (12) and (13) are coupled through the coordinate ρ so can not be solved independently.

Taken on its own, (12) represents a displaced harmonic oscillator at radius $\rho_T = k_H/(\mu\omega_H^2)$, whose solutions can be written in terms of Hermite Polynomials. It is a reasonable assumption that the rotational motion and the additional distortion will not change the radius of the trough and hence this solution to the vibrational equation. We can therefore set $\rho = \rho_T$ in (13) and solve it independently from (12).

3. Solutions to the rotational differential equations

In order to understand the effects of the additional distortion, it is first useful to look at the effective potential U_{eff} evaluated at $\rho = \rho_T$ for distortions in different directions ν. From this, we can see that a distortion in the θ direction will cause a maximum energy-lowering of $-|w_\theta|/2$ for w_θ positive or $-|w_\theta|$ for w_θ negative. Furthermore, as W_θ only contains the angle θ, the minimum-energy points occur for all values of ϕ (for both signs of w_θ). Physically, this means that a θ–type distortion will result in one of the two pseudorotations being converted into a vibration. However, distortions in the other four directions of coordinate space ($\nu = \epsilon, 4, 5, 6$) all cause a maximum energy lowering of $-\sqrt{3}|w_\nu|/2$, independent of the sign of w_ν. Also, the minimum-energy points occur for specific values of θ and ϕ, which physically means that both pseudorotations have been converted into vibrations.

3.1. Distortion in θ direction

When we consider a distortion in the θ direction only, we find that for $w_\theta > 0$, a minimum in U_{eff} occurs at $\theta = \pi/2$ and a maximum at $\theta = 0$. For $w_\theta < 0$, this situation is reversed with the minimum occurring at $\theta = 0$ and the maximum at $\theta = \pi/2$. The depth of the minimum increases as the magnitude of the JT coupling k_H increases.

Separated solutions to Eq. (13) can be sought in terms of a product of functions $\Theta(\theta)$ and $\Phi(\phi)$ of the angles θ and ϕ respectively. A general form for the rotational wave function ψ_R will then be a linear combination of the products. From the Equation in ϕ

and knowledge (from the analysis of U_{eff}) that we do not expect $|\psi_R^2|$ to depend upon ϕ, we deduce that $\Phi(\phi)$ can be represented by terms proportional to $\exp(\mathrm{i}m\phi)$, with m being an integer.

By applying the change of variable $x = \cos\theta$, the equation in Θ becomes

$$\frac{d^2\Theta(x)}{dx^2} - \frac{2x}{1-x^2}\frac{d\Theta(x)}{dx} + \left[\frac{2a_\theta(1-3x^2)+c_\theta}{1-x^2} - \frac{m^2}{(1-x^2)^2}\right]\Theta(x) = 0, \tag{14}$$

with $a_\theta = 3\mu w_\theta \rho_T^2/(2\hbar^2)$ and $c_\theta = 6\mu\rho_T^2 E_{R\theta}/\hbar^2$. This is a standard differential equation whose solutions are spheroidal functions. The spheroidal functions can be expressed as a linear combination of Associated Legendre polynomials P_l^m, where l and m are the usual angular momentum quantum numbers [22]. Therefore, for any given value of m, we can write[22]

$$\psi_R(\theta,\phi) = \sum_{s=0,1}^{\infty\prime} C_s^m Y_{m+s}^m(\theta,\phi). \tag{15}$$

where $s = l - m$ and the prime indicates that the sum is from zero except for $m = 0$ where the sum is from 1. The Y_{m+s}^m are spherical harmonics and the C_s^m are coefficients whose values can be found recursively after solving a transcendental equation for the eigenvalues [22]. Different solutions exist for odd and even values of l. Also, the transcendental equation results in multiple solutions for each given value m. The solutions for a given value of m will be labeled in order of increasing energy by an index n, where $n = 0$ corresponds to the state with lowest energy.

To render the solutions physical, we require that Ψ_g be periodic under the transformations $\theta \rightarrow \pi + \theta$ and $\phi \rightarrow \phi + 2\pi$ [20]. Under this transformation, ψ_g changes sign, so to preserve the overall sign of Ψ_g, ψ_R and consequently $\Theta(\theta)$ should change sign. As in the $T \otimes h$ problem with no distortion, l must be odd to satisfy the above conditions. Furthermore, for the wavefunctions to satisfy these conditions and be physically acceptable requires that m be odd for $w_\theta > 0$ and even for $w_\theta < 0$.

The wavefunctions can be computed numerically for specific values of k_H and w_θ. Convergence is achieved by including the first 25 terms in the sum over s. For the lowest states (i.e. with $m = 1$ for $w_\theta > 0$ and $m = 0$ for $w_\theta < 0$), $|\psi_R|^2$ is found to be a Gaussian-like function of θ centred over the position of minimum energy. The wavefunction becomes much more strongly localised around the position of minimum energy at strong JT coupling than at weak coupling. For example, with $w\theta = 0.5\hbar\omega_H$, $|\psi_R|^2$ is approximately a Gaussian with standard deviation $\sigma \approx 0.52$ for $k_H = \hbar\omega_H$, whereas σ is less than half this at ≈ 0.24 for $k_H = 10\hbar\omega_H$. This behaviour is to be expected as the potential minimum will be deeper for stronger JT couplings.

3.2. Distortion in ϵ, 4, 5 or 6 directions

The minima in U_{eff} for distortions in directions $\nu = 4, 5$ and 6 are at the same depth as minima in the ϵ direction for an equivalent magnitude distortion. It is therefore sufficient to consider the effects of W_ϵ only. For the rotational wave function to be

physically acceptable and to be invariant under the transformations $\phi \rightarrow \phi + 2\pi$ and $\theta \rightarrow \theta + \pi$, we require m to be odd for an ϵ–type distortion of either sign. It should be noted that m must also be odd for a 6–type distortion, but that it must be even for a 4 or 5–type distortion.

Unlike with a θ-type distortion, minima in U_{eff} for an ϵ-type distortion occur at particular values of ϕ as well as particular values of θ. More specifically, they occur at $\theta = \pi/2$, and $\phi = \{\pi/2, 3\pi/2\}$ for $w_\epsilon > 0$ and at $\phi = \{0, \pi\}$ for $w_\epsilon < 0$. The form of the potential for $w_\epsilon < 0$ is exactly the same as that for a positive value of w_ϵ of the same magnitude except for a displacement of the values of ϕ by $\pi/2$. Therefore, the expected rotational wave functions will also be identical except for the displacement of ϕ values, and the energies of the rotational wave functions will be exactly the same. This means that it is only necessary to consider the magnitude of w_ϵ and not its sign.

The differential equation for a distortion in the ϵ direction is non-separable, unlike for the θ direction. However, we can still seek a solution in the form of a linear combination of products of functions $\Phi(\phi)$ and $\Theta(\theta)$. To determine the form of those functions, we note that the term W_ϵ can be written in terms of the spherical Harmonics $Y_2^{\pm 2}(\theta, \phi)$ as:

$$\frac{w_\epsilon \sqrt{3}}{2} \sin^2\theta \cos 2\phi = w_\epsilon \sqrt{\frac{2\pi}{15}} (Y_2^{-2}(\theta, \phi) + Y_2^2(\theta, \phi)). \tag{16}$$

The conditions on Φ are such that we seek a solution of the form

$$\Psi_R = \sum_s C_s^m P_{m+s}^m (\cos\theta) \begin{cases} \sin m\phi & w_\epsilon > 0 \\ \cos m\phi & w_\epsilon < 0 \end{cases} \tag{17}$$

where the C_s^m are coefficients to be determined. We can substitute this and Eq. (16) into Eq. (13), multiply by $Y_{l'}^{m'*}$ and integrate over θ and ϕ. The integrals can be expressed in terms of Wigner $3j$–symbols (or Clebsch-Gordan coefficients) which vanish unless $l = l'$ or $l = l' \pm 2$, and $m' = m \pm 2$. This defines recursion relations, which will not be explicitly written here due to their complex form.

The rotational wave functions can again be computed numerically. In this case, 50 terms are required to ensure convergence. Results for $|\psi_R|^2$ are given in Figs. 3.2(a) and 3.2(b) for $k_H = \hbar\omega_H$ and $w_\epsilon = \pm 0.5\hbar\omega_H$ respectively. As expected, maxima in the lowest rotational function occur at angles giving minima in U_{eff}. The average of $|\psi_R|^2$ also occurs at these minima for the next-lowest rotational function. It should be noted that W_θ could have been written in terms of $Y_2^0(\theta, \phi)$ and solved in the same manner as the ϵ term, although this was not done as the differential equation has well-known solutions.

3.3. Distortion in other directions

So far, we have considered symmetry-lowering distortions in the directions of coordinate space we have defined to be θ, ϵ, 4, 5 and 6. However, it is obviously possible to have distortions in directions that are a linear combination of these directions. The general

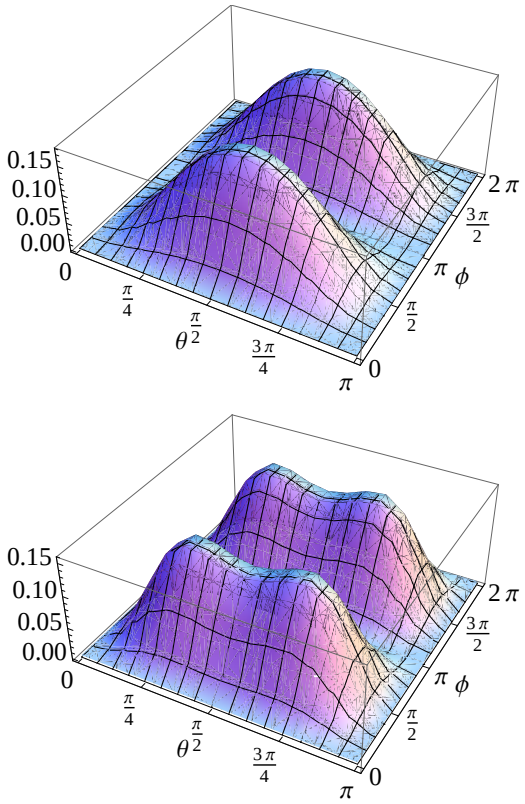

Figure 1. (Color online) Plots the square of the rotational wavefunction, $|\psi_R|^2$, for (a) the ground state, and (b) the next-lowest state with $k_H = \hbar\omega_H$ and with an ϵ–type distortion $w_\epsilon = 0.5\hbar\omega_H$.

case with a distortion in a linear combination of all five directions is complicated due to the high dimensionality of the problem. Therefore, we will only consider distortions in a linear combination of two of the basic directions above. This will be sufficient to illustrate the complexity of the problem.

We will consider a (dimensionless) combination

$$E_{\nu\lambda} = W_\nu \cos\beta/w_\nu + W_\lambda \sin\beta/w_\lambda \tag{18}$$

of two different distortions for all pairs of values of ν and λ taken from the set $\{\theta, \epsilon, 4, 5, 6\}$. Calculating the minimum in the energy of this factor as the angles θ and ϕ are varied allows us to examine the effect of varying the contribution from two different distortions for a fixed overall magnitude of distortion. We find that the results fall into four categories. Firstly, the energy of the combinations W_ϵ–W_6, W_4–W_5, W_4–W_6 and W_5–W_6 are all independent of the mixing angle β, taking the value $-\sqrt{3}/2$ found for the separate components $\{\epsilon, 4, 5, 6\}$. However, the same is not true for other combinations of these four directions. For $\nu = \epsilon$ and $\lambda = 4$, the minimum energy is a minimum of $\sqrt{3}\cos\beta/2$ and the value of $E_{\nu\lambda}$ with $\phi = \pi/2$ and $\tan 2\theta = 2\tan\beta$, as shown in Fig. 2(a). For $\nu = \epsilon$ and $\lambda = 5$, the minimum energy is a minimum of $-\sqrt{3}\cos\beta/2$ and the value of $E_{\nu\lambda}$ with $\phi = \pi/2$ and $\tan 2\theta = -2\tan\beta$. The result is

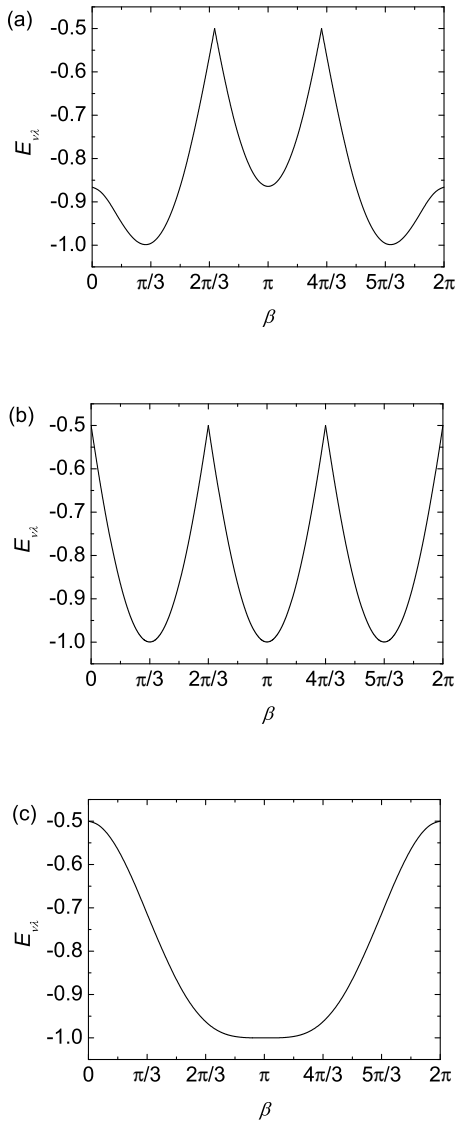

Figure 2. Variation in $E_{\nu\lambda}$ (dimensionless units) as a function of the angle β for (a) $\nu = \epsilon$ and $\lambda = 4$ (results for $\lambda = 5$ are the same if the x-axis runs from $\beta = \pi$ to 3π), (b) $\nu = \theta$ and $\lambda = \epsilon$ or 6, (c) $\nu = \theta$ and $\lambda = 4$ or 5.

the same as in Fig. 2(a) but where the x–axis is taken to run from $\beta = \pi$ to $\beta = 3\pi$ rather than from $\beta = 0$ to π.

As we have already found that the results for a distortion in the direction θ are different to those in the other four directions we have considered, it is not surprising that the results when a θ–type distortion is mixed with a distortion in another direction are also different. For combinations $\nu = \theta$ and $\lambda = \epsilon$ or 6, the minimum energy for a given mixing angle β is the minimum of $\{\cos\beta, \cos(\beta + 2\pi/3), \cos(\beta + 4\pi/3)\}$, as shown in Fig. 2(b). The remaining cases are those of $\nu = \theta$ and $\lambda = 4$ and 5. Here, the result is the minimum root of $E_{\nu\lambda}$ with $\tan 2\theta = 2\tan\beta/\sqrt{3}$, as shown in Fig. 2(c).

One feature of all of our results is that the energy change due to a distortion of magnitude w always lies between $-w/2$ and $-w$. The maximum energy change of $-w$ occurs for a θ–type distortion with w_θ negative, as well as for certain other combinations of our basic distortion directions. Similarly, the smallest energy change for a fixed magnitude of distortion w occurs for a θ–type distortion with w_θ positive and other combinations of directions.

The results above show that the topology of the APES when uniaxial distortions are applied is rather complex. However, this is not obvious without a detailed examination of the potential energy terms. Linear JT coupling alone produces a trough of equal minimum-energy points that can be mapped onto the surface of a two-dimensional sphere [14]. However, as we have seen, the effect to the sphere of different symmetry-lowering distortions are far from equivalent.

4. Energies of rovibronic states

To understand how the $T \otimes h$ JT system behaves under a symmetry-lowering distortion, we have to evaluate the total energy of the system. In general, this can be written as

$$E_h = \frac{\int \Psi'_g(\theta', \phi'\gamma')\mathcal{H}\Psi_g(\theta, \phi\gamma)d\Omega d\Omega'}{\int \Psi'_g(\theta', \phi'\gamma')\Psi_g(\theta, \phi\gamma)d\Omega d\Omega'} \tag{19}$$

where $\Psi_g^{'}$ and Ψ_g are the total wave functions on the LAPES given by Eq. (10), evaluated at different points on the trough of minimum-energy points, and $d\Omega = \sin\theta d\theta d\phi$ and $d\Omega' = \sin\theta' d\theta' d\phi'$ are elements of volume. The numerator and denominator are therefore both four dimensional integrals.

In order to display the results, it is convenient to define a coupling constant $K_H = k_H\sqrt{\hbar/\mu\omega_H}$, which has dimensions of energy. Also, in order to distinguish the effects of the additional distortion from the effect of the JT coupling alone, rather than considering E_h alone it is more useful to look at the term $(E_h + E_{JT})/\hbar\omega_H$ where [14, 21] $E_{JT} = K_H^2/(2\hbar\omega_H)$ is the JT energy, i.e. the energy of the lowest point on the LAPES when no additional distortion is present.

In this paper, we will only consider the ground vibrational state with different rotational levels, although the calculations can be extended to higher vibrational states. In this case, we can extract out the zero-point energy for zero vibronic coupling and write

$$\frac{E_h + E_{JT}}{\hbar\omega_H} = \frac{5}{2} + \frac{3K_H^2}{4}I(K_H, w), \tag{20}$$

with

$$I(K_H, w) = \frac{\int Z^3 \mathrm{e}^{\frac{3K_H^2}{4}(Z^2-1)} e^{\mathrm{i}m(\phi'-\phi)}\psi'_R\psi_R d\Omega d\Omega'}{\int Z \mathrm{e}^{\frac{3K_H^2}{4}(Z^2-1)}\mathrm{e}^{\mathrm{i}m(\phi'-\phi)}\psi'_R\psi_R d\Omega d\Omega'} - 1 \tag{21}$$

for a given rotational state. Z is the electronic overlap between two points on the trough given by:

$$Z = \cos\theta'\cos\theta + \sin\theta'\sin\theta\cos(\phi' - \phi). \tag{22}$$

ψ'_R and ψ_R are the rotational wave functions at points $(\theta', \phi', \gamma')$ and (θ, ϕ, γ) respectively. $I(K_H, w)$ can be evaluated for specific values of m.

As an alternative to the calculation above, low-lying energy levels can be found numerically using a recursive Lanczos technique. [23, 24, 25, 26, 27] An advantage of this method is that it automatically includes both rotational and vibrational excitations. However, applying this technique to our system brings technical problems. To avoid degenerate 'repeated' eigenvectors, the number of starting vectors must be set to fifteen or more, but when this is done computational problems arise. We will not consider this method any further in this paper.

4.1. Distortion in the θ direction

First of all we will consider results for the rotational states associated with the ground vibrational state in the limit when the θ-type distortion tends to zero in order to confirm that our method gives results consistent with previous work. In this limit, we expect to obtain states which are degenerate at an energy of $1.5\hbar\omega_H$ in strong JT coupling, representing the presence of three vibrations and two (pseudo)rotations. In zero JT coupling, we expect energies of $2.5\hbar\omega_H$, $3.5\hbar\omega_H$, $4.5\hbar\omega_H$ etc, [21] corresponding to a five-dimensional harmonic oscillator. Each curve will have a degeneracy $l = 2m + 1$, where l is odd, such that the lowest curve is for $l = 1$, the next curve for $l = 3$ etc.

For any given value of m, we can calculate rotational levels for the zero distortion case using our θ–type rotational wave functions by setting the distortion to zero. Fig. 3(a) shows the value of $(E_h + E_{JT})/\hbar\omega_H$ for the first three rotational states ($n = 0$, 1 and 2) as calculated using either the wave functions appropriate to positive w_θ and with $m = 1$, or using the wave functions appropriate to negative w_θ and with $m = 0$. It can be seen that the results do indeed show the behavior that we expect in this limit. Note that results have not been given for $K_H/\hbar\omega_H < 1$ as the wave functions are not appropriate for weak JT couplings. However, our results for $K_H/\hbar\omega_H = 1$ are consistent with results for states tending to the expected limits of $2.5\hbar\omega_H$, $3.5\hbar\omega_H$ and $4.5\hbar\omega_H$ as $K_H \to 0$.

Next we consider the effects of a θ–type distortion. This will lift the m-fold degeneracy of the rotational levels. Figs. 3(b) and 3(c) give results for the lowest three rotational levels ($n = 0$ to 2) of the set $m = 0$ for $w_\theta < 0$, and the set $m = 1$ for $w_\theta > 0$. In the latter case, $m = -1$ gives identical results to $m = 1$. Fig. 3(b) gives the results for a weak distortion of $|w_\theta| = 0.5\hbar\omega_H$, and Fig. 3(c) gives the results for a strong distortion of $|w_\theta| = 5\hbar\omega_H$. As expected, the results with a distortion are lower than those with no distortion. Furthermore, the lowering for $w_\theta < 0$ is approximately twice the lowering for $w_\theta > 0$. This is also expected from the potential U_{eff}, which shows that the minimum is lowered twice as much for a negative distortion as it is for a positive distortion of the same magnitude. This result is easiest to observe in Fig. 3(c) where the effects of the distortion are much larger than in Fig. 3(b).

While the difference in energy between the results with positive and negative

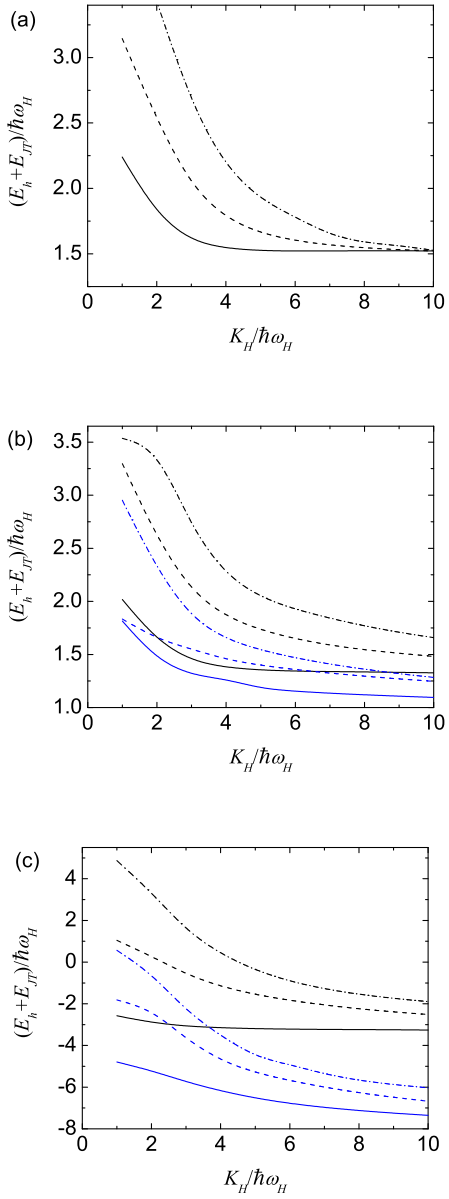

Figure 3. (Color online) Plot of $(E_h + E_{JT})/(\hbar\omega_H)$ versus $K_H/\hbar\omega_H$ for a distortion applied in the θ direction for (a) no symmetry-lowering distortion ($w_\theta \to 0$), (b) weak distortion ($w_\theta = \pm 0.5\hbar\omega_H$), and (c) strong distortion ($w_\theta = \pm 5\hbar\omega_H$). In all plots, the solid lines are rotational levels $n = 0$, the dashed lines are for $n = 1$ and the dot–dash lines are for $n = 2$. The lowest three (blue) lines for $K_H/\hbar\omega_H = 10$ are the $m = 0$ levels for negative w_θ, and the highest three (black) lines are the $m = \pm 1$ levels for positive w_θ.

distortions can be explained by examining U_{eff}, the absolute values of the energies can not be explained without performing the detailed calculation. Also, U_{eff} does not explain why the results for different values of n with a distortion do not reach the same value as each other in strong JT coupling until much larger values of $K_H/\hbar\omega_H$ than with no distortion. These features can be attributed to changes in the form of the rotational wave function. The effect of the distortion is to select out a circle of minimum-energy points characterized by the angle ϕ for a fixed value of θ (namely $\theta = \pi/2$ for $w_\theta > 0$ and $\theta = 0$ for $w_\theta < 0$), whereas for no distortion all values of the angle θ also result in the minimum energy. Therefore one of the two pseudorotations for zero distortion is converted into a vibration with a strong distortion. As a consequence, there is a significant change in the rotational wave function as the strength of the distortion increases, from one which is not localised in θ to one which is. In the strong distortion limit, the wave function is really one for a vibration in this coordinate rather than a function for a rotation.

The energies in Fig. 3 were calculated by integrating over all points $\{\theta, \phi\}$ that form the trough of minimum-energy points with no distortion. However, as θ is fixed at a specific value for a strong distortion, a good approximation to the energy for large distortions can be obtained if we fix θ to this value and only integrate over ϕ. This reduces the integrals from four dimensions to two. When this is done, we find that the results are very similar to those with the full four-dimensional integrals. For example, results for $|w_\theta| = 5\hbar\omega_H$ only differ by $\approx 0.01\hbar\omega_H$. Hence a good approximation to the energies for a strong distortion can be found by integrating over two dimensions only.

4.2. Distortion in directions $\{\epsilon, 4, 5, 6\}$

As mentioned in Section 3.2, the minimum in U_{eff} for a distortion W_ν is at the same value for all directions $\nu = \epsilon, 4, 5$ and 6, and also at the same value irrespective of the sign of w_ν. As a consequence, we expect the energies of the rovibronic states to be the same for all of these cases. In fact, this provides a useful check on the method of calculation. From our calculations, we find agreement to at least $10^{-5}\hbar\omega_H$ for distortions w_ν with the different values of ν above, and for equivalent positive and negative distortions.

As mentioned previously, only states with m even are allowed for the w_4 and w_5-type strains, whereas m must be odd for w_ϵ and w_6-type strains. Fig. 4 shows the average energy of the lowest three rotational states of the lowest allowed value of m, namely for $m = \pm 1$ for $\nu = \epsilon$ or 6 and $m = 0$ for $\nu = 4$ or 5. The upper (dashed blue) results are for a weak distortion of $|w_\nu| = 0.5\hbar\omega_H$, and the lower (solid black) results are for a strong distortion of $|w_\nu| = 5\hbar\omega_H$. As expected, Fig. 4 shows that the effect of a stronger distortion is larger than that of a weaker distortion.

For a strong distortion in the θ direction, we found that a good approximation to the energies E_h can be obtained by integrating over the angles that define the minimum-energy points only. The same is true here, although the result is even simpler as the minimum in energy occurs for fixed angles θ and ϕ. Therefore it is not necessary to

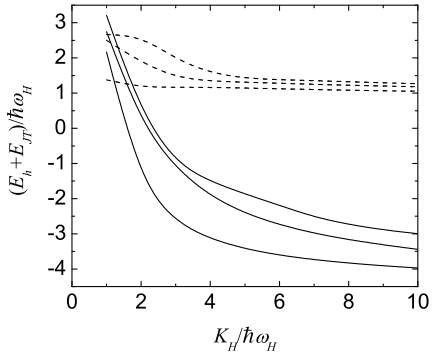

Figure 4. Plot of $(E_h + E_{JT})/(\hbar\omega_H)$ versus $K_H/\hbar\omega_H$ for a distortion w_ν where $\nu = \epsilon, 4, 5$ or 6. The lower (solid black) curves are the lowest three energies for the lowest allowed value of m and $w_\nu/\hbar\omega_H = \pm 5$, and the upper (dashed blue) curves are the corresponding energies for $w_\nu/\hbar\omega_H = \pm 0.5$.

evaluate any integrals at all.

4.3. Comparison of different directions of distortion

We can investigate the effect of different distortions further by plotting results at a fixed coupling constant K_H as a function of the magnitude of the distortion. Fig. 5 shows results for $K_H/\hbar\omega_H = 10$. The solid line is for w_θ positive, the dot-dashed line is for w_θ negative, and the dashed line is for $|w_\nu|/\hbar\omega_H$ with $\nu = \epsilon, 4, 5$ or 6.

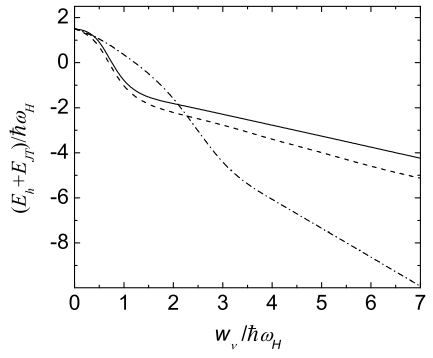

Figure 5. Plot of $(E_h + E_{JT})/(\hbar\omega_H)$ versus $|w_\nu|/\hbar\omega_H$ for a distortion w_ν where $\nu = \epsilon, 4, 5$ or 6. The solid curve is for w_θ positive, the dot-dash line is for w_θ negative, and the dashed line is for $|w_\nu|/\hbar\omega_H$ with $\nu = \epsilon, 4, 5$ or 6.

The results can be interpreted as follows. As already stated, there is a two-dimensional trough of minimum-energy points in the APES when there is no distortion. [14] The motion of the system consists of a pseudorotation (i.e. a rotation of a distortion) in two directions around the trough, and vibrations in three directions perpendicular to

the trough. When a small θ-type distortion is introduced, a circle of points on this sphere of minimum-energy points will become lower in energy than the other points, producing a shallow one-dimensional trough. One of the two pseudorotations will then become a hindered rotation, whereby a distortion still rotates but there is a preference for a particular distortion. As the strength of the distortion increases further, the hindered rotation will turn into a vibration about the minimum-energy point. However, other points on the APES will still influence the overall motion at these strengths. When the distortion becomes very strong, the motion will consist entirely of four vibrations and a pseudorotation. Further increases in the strength of the distortion lower the energy of the one-dimensional trough, but will not alter which points contribute to the motion.

When a small distortion in any of the directions ϵ, 4, 5 or 6 is introduced, a single point on the sphere of minimum-energy points will become lower in energy than the other points, producing a shallow potential well. Both of the pseudorotations will become hindered rotations, which turn into vibrations as the strength of the distortion increases further. Further increases in the strength of the distortion lower the energy of the potential well but, as with the θ-type distortion, will not alter which points contribute to the motion.

As a consequence of the above interpretation, we expect curves of energy against the strength of the distortion to become linear for strong distortions in any direction, with a negative gradient (to indicate that increasing the distortion strength lowers the energy) whose magnitude is closely related to the value of the energy lowering due to the distortion terms. From Section 3.3, we can see that this would predict gradients of -0.5 and -1 for positive and negative θ–type distortions respectively, and of $-\sqrt{3}/2 \approx -0.866$ for an ϵ–type distortion. Fig. 5 shows that for strong distortions, the variation in energy is indeed linear, with gradients of -0.485, -1.285 and -0.588 for the three cases above respectively. This indicates that, for sufficiently large distortions, there is indeed a correlation between the gradients and the energy lowering due to the distortion terms.

5. Conclusion

In this paper, we have examined a linear $T \otimes h$ JT system subject to an additional symmetry-lowering distortion that can be written in terms of the electronic operators σ_λ used to describe the intramolecular JT interaction. Physically, this situation could represent a single C_{60}^- ion subject to an external stress. However, a situation which is likely to be of much greater practical importance is a cluster or continuous solid of interacting C_{60}^- ions, such as found in the AC_{60} alkali-doped fullerides (where A is an alkali metal). In a molecular field approximation, the effect on a given C_{60}^- ion of co-operative JT interactions with other C_{60}^- ions can be modelled using such terms. The co-operative interactions will result in real distortions of the icosahedral (I_h) cage of the C_{60} molecule to a lower symmetry.

There is currently much interest in the use of C_{60} and its derivatives adsorbed onto

surfaces, where there is the possibility of transferring some of the unique properties of C_{60} to a solid interface. This could have important technological implications relating to coatings and other surface modifications [28]. Being able to control the properties of organic materials leads to the possibility of exploitation in future nanostructured devices, with potential applications ranging from electronics to medicine [29]. In general, the interaction of a C_{60} anion with a surface will also lead to a distortion of a system. It has therefore been suggested that surface interactions could be written (again phenomenologically), at least to a first approximation, in terms of an expansion in the σ_λ for an h mode, which would result in a similar symmetry-lowering distortion to that used to describe co-operative JT effects [30]. However, to do this, the relevant operators must have a symmetry appropriate to that of both the adsorbed molecule and of the surface. This will depend upon the symmetry of the site at which the molecule is adsorbed. Therefore, it may or may not be appropriate for a real situation. If this is not the case for a given surface interaction, then it will be necessary to construct an alternative form for $\mathcal{H}_{s\lambda}$. Nevertheless, an analysis similar to that used here could then follow.

The results of our calculations give the change in energy of the vibronic states of the C_{60}^- ion due to the introduction of symmetry-lowering terms. It might be hoped that the results could be predicted, at least approximately, from the rather simpler analysis of the effective potential, U_{eff}. However, this is not found to be the case due to significant changes in the form of the wave function when a distortion is introduced. It is nevertheless possible to simplify the calculations for strong distortions by only integrating over angles that result in minimum-energy positions (for a θ-type distortion) or by evaluating the energy at fixed angles (for an ϵ, 4, 5 or 6-type distortion).

Distortions related to the normal mode displacements of an h mode are possible in five different mutually-orthogonal directions, or in any linear combination of those directions. In the linear $E \otimes e$ JT system, the LAPES contains a trough of equivalent minimum-energy points, known as the Mexican hat potential. It has previously been found that when an additional distortion is applied, the results do not depend upon the direction of the distortion [31]. As the linear $T \otimes h$ problem also contains a trough of minimum-energy points, it might be expected that results for distortions in different directions would also be equivalent. However, this is found to be not the case. A distortion in the θ direction is different from that along any of the other four symmetry directions (ϵ, 4, 5 and 6), which are however equivalent amongst themselves. Also, a distortion in the positive θ direction is different to that in a negative θ direction, whereas for the other four directions the results do not depend on the sign of the distortion. When a linear combination of the five symmetry directions is considered, a complex set of results is obtained, with energies ranging from that of the positive θ-direction to that of the negative θ-direction. The rich nature of the results arises from the high dimensionality of the problem. Care must be taken when extrapolating results from simpler physical situations involving lower dimensions. The icosahedral symmetry of the C_{60} molecule is the highest point-group symmetry found in nature. Our results are

an example of where the high symmetry produces features not seen in systems of lower symmetry. Other cases where the high symmetry produces unexpected results includes the $H \otimes h$ JT system, where non-simple reducibility of the product $H \otimes H$ can result in a singlet ground state rather than the expected five-fold state [32, 33].

References

[1] Gunnarsson O. *Rev. Mod. Phys.*, 69:575, 1997.

[2] Haddon R C. *Accounts Chem. Res.*, 25:127–133, 1992.

[3] Aldersey-Williams H. *The most beautiful molecule: The discovery of the BuckyBall*. John Wiley and sons, New York, 1995.

[4] Shi W, Zhou W, Cao Y, Li B, Zhang Z, and Teng Y. *J. Mol. Struct.*, 546:11–15, 2001.

[5] Sundar C S, Gupta R, Premila M, Bharathi A, Hariharan Y, and Sood A K. *J. Phys. Chem. Solids*, 63:1639–1646, 2002.

[6] Lappas A, Kosaka M, Tanigaki A, and Prassides K. *J. Am. Chem. Soc.*, 117:7560–7561, 1995.

[7] Fally M and Kuzmany H. *Phys. Rev. B*, 56:13861, 1997.

[8] Chauvet O, Oszlànyi G, Forro L, Stephens P W, Tegze M, Faigel G, and Jànossy A. *Phys. Rev. Lett.*, 72:2721–2724, 1994.

[9] Remova A A, Levashov V A, Shpakov V P, Paek U H, and Belosludov V R. *Synthetic metals*, 86:2391–2392, 1997.

[10] Blank V D, Buga S G, Serebryanaya N R, Dubitsky G A, Sulyanov S N, Popov M Yu, Denisov V N, Ivlev A N, and Mavrin B N. *Phys. Lett. A*, 220:149, 1996.

[11] Ceulemans A, Chibotaru L F, and Cimpoesu F. *Phys. Rev. Lett.*, 78:3725–3728, 1997.

[12] Stephens P W, Mihaly L, Lee P L, Whetten R L, Huang S M, Kaner R, Deiderich F, and Holczer K. *Nature*, 351:632, 1991.

[13] Dresselhaus M S and Dresselhaus G. *Annu. Rev. Mater. Sci.*, 25:487–523, 1995.

[14] Chancey C C and O'Brien M C M. *The Jahn-Teller effect in C_{60} and other icosahedral complexes*. Princeton University Press, Princeton, 1997.

[15] Kaplan M D and Vekhter B G. *Cooperative phenomena in Jahn-Teller crystals*. Plenum Press, New York, 1995.

[16] Dunn J L. *Phys. Rev. B*, 69:064303, 2004.

[17] Feiner L F. *J. Phys. C: Solid State Phys.* , 15:1495, 1982.

[18] M. C. M. O'Brien. The energy-level structure of a jahn-teller system strongly coupled to many modes of vibration. *Journal of Physics C: Solid State Physics*, 16(1):85–106, —1983—.

[19] Dunn J L and Bates C A. Analysis of the $t_{1u} \otimes h_g$ jahn-teller system as a model for c_{60} molecules. *Phys. Rev. B*, 52(8):5996–6005, 1995.

[20] O'Brien M C M. *Phys. Rev. B*, 53:3775, 1996.

[21] Dunn J L, Eccles M R, Liu Y M, and Bates C A. *Phys. Rev. B*, 65:115107, 2002.

[22] Abramowitz M and Stegun I A. *Handbook of mathematical functions*. Dover, New York, 1964.

[23] Bevilacqua G, Martinelli L, and Pastori G P. *Revista Mexicana de Física*, 44:15, 1998.

[24] Van Loan C F and Golub G H. *Matrix Computations*. John Hopkins University Press, Baltimore, 1996.

[25] Simon H D. *Linear Algebra and its Applications*, 61:101, 1984.

[26] Parlett B N and Scott D S. *Math. Comput.*, 33:217, 1979.

[27] Bai Z J, Day D, and Ye Q. *Siam J. Matrix Anal. Appl.*, 20:1060, 1999.

[28] Bonifazi D, Enger O, and Diederich F. *Chem. Soc. Rev.*, 36(2):390–414, 2007.

[29] Zhang E Y and Wang C R. *Curr. Opin. Colloid Interface Sci.*, 14(2):148–156, 2009.

[30] Hands I D, Dunn J L, Rawlinson C S A, and Bates C A. Jahn-teller effects in molecules on surfaces with specific application to c_{60}. In Köppel H, Barentzen H, and Yarkony D R, editors,

The Jahn-Teller effect Advances and Perspectives, Springer Series in Chemical Physics, page In Press. Springer-Verlag, 2009.

[31] Moujaes E A, Dunn J L, and Bates C A. *J. Mol. Struct.*, 838:238–243, 2007.

[32] Moate C P, O'Brien M C M, Dunn J L, Bates C A, Liu Y M, and Polinger V Z. *Phys. Rev. Lett.*, 77(21):4362–4365, 1996.

[33] DeLosRios P, Manini N, and Tosatti E. *Phys. Rev. B*, 54(10):7157–7167, 1996.